

### Supporting Information

#### Mechanism of a-Ga<sub>2</sub>O<sub>3</sub>/MoS<sub>2</sub> Heterojunction for High-Performance Self-Powered Solar-Blind Photodetection and Imaging

Lai Yuan<sup>#</sup>, Quancai Yue<sup>#</sup>, Hong Zhang, Di Pang, Guoping Qin, Honglin Li<sup>\*</sup>, Yan Tang<sup>\*</sup>, Lijuan Ye<sup>\*</sup> and Wanjun Li

Chongqing Key Laboratory of Photo-Electric Functional Materials and Laser Technology, College of Physics and Electronic Engineering, Chongqing Normal University, Chongqing, 401331, People's Republic of China

<sup>#</sup> These authors contributed equally to the work.

<sup>\*</sup>E-mail: lin@cqnu.edu.cn (H. Li), tytang2016@163.com (Y. Tang), yelj@cqnu.edu.cn (L. Ye)

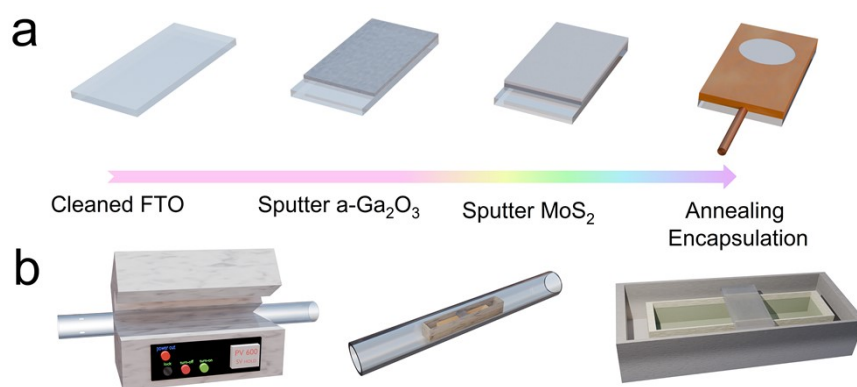
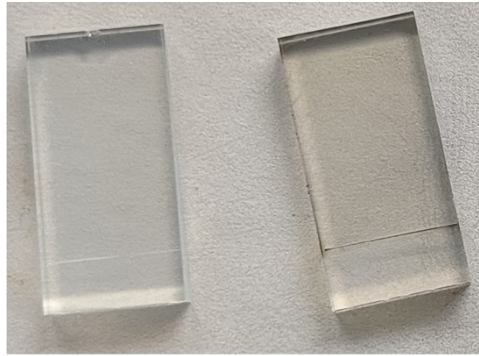


**Figure S1** (a) Fabrication process of the a-Ga<sub>2</sub>O<sub>3</sub>/MoS<sub>2</sub>; (b) Schematic illustration of the high-temperature sulfurization process.



a-Ga<sub>2</sub>O<sub>3</sub>

a-Ga<sub>2</sub>O<sub>3</sub>/MoS<sub>2</sub>

**Figure S2** Left panel: sample with only a-Ga<sub>2</sub>O<sub>3</sub> sputtered on FTO; Right panel: sample with a-Ga<sub>2</sub>O<sub>3</sub>/MoS<sub>2</sub> heterostructure sputtered on FTO.

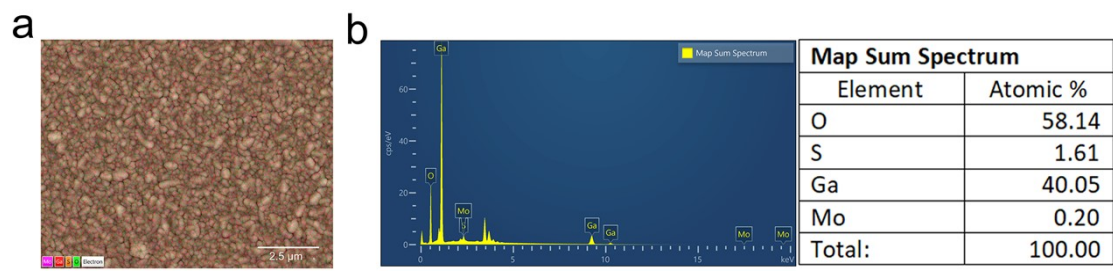


**Figure S3** (a) EDS image of the a-Ga<sub>2</sub>O<sub>3</sub>/MoS<sub>2</sub> heterojunction device; (b) Corresponding elemental mapping spectra and quantitative content analysis for selected area (a).

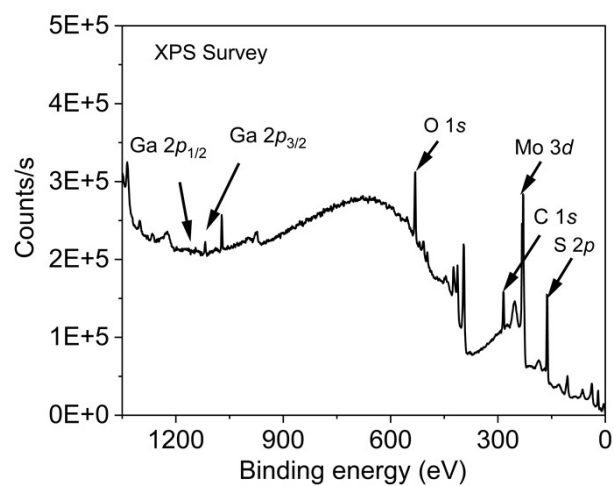


**Figure S4** XPS survey spectrum of the a-Ga<sub>2</sub>O<sub>3</sub>/MoS<sub>2</sub> heterojunction device surface.

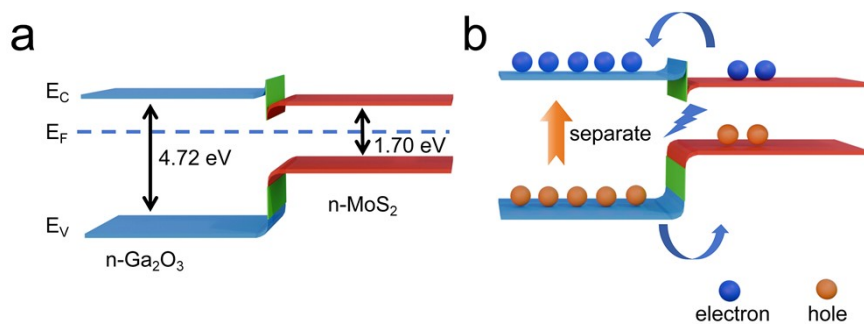


**Figure S5** (a) Schematic energy band diagram illustrating the band bending after Fermi level alignment between  $n\text{-Ga}_2\text{O}_3$  and  $\text{MoS}_2$ . (b) Schematic illustration of carrier separation and transport under 254 nm illumination.

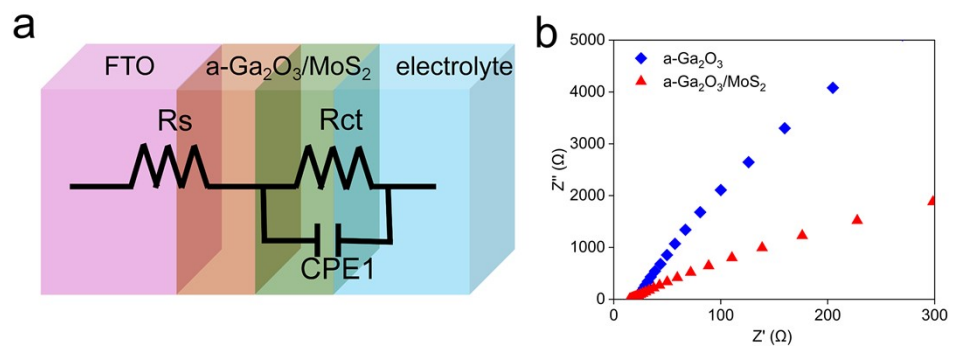


**Figure S6** (a) Equivalent circuit diagram used for fitting the Mott-Schottky measurements; (b) Fitted Mott-Schottky plot.

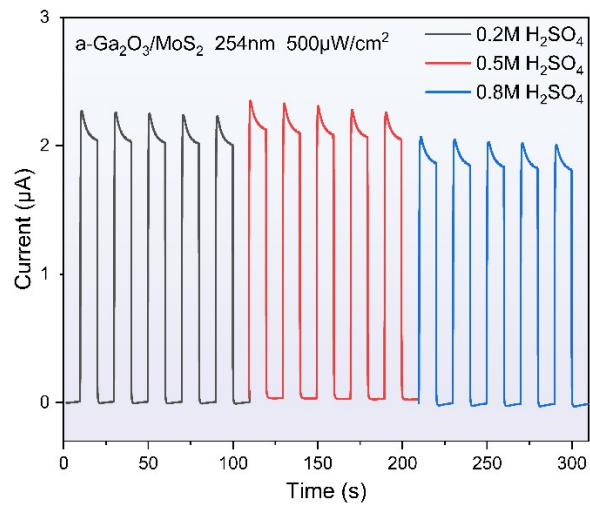


**Figure S7** I-t curves of the a-Ga<sub>2</sub>O<sub>3</sub>/MoS<sub>2</sub> ultraviolet photodetector measured in H<sub>2</sub>SO<sub>4</sub> electrolytes with concentrations of 0.2, 0.5, and 0.8 M.

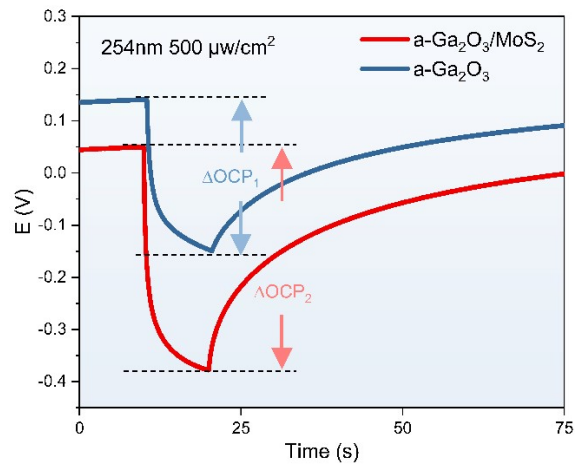


**Figure S8** OCP profiles of the a-Ga<sub>2</sub>O<sub>3</sub>/MoS<sub>2</sub> heterojunction versus the pristine a-Ga<sub>2</sub>O<sub>3</sub> device under intermittent illumination.

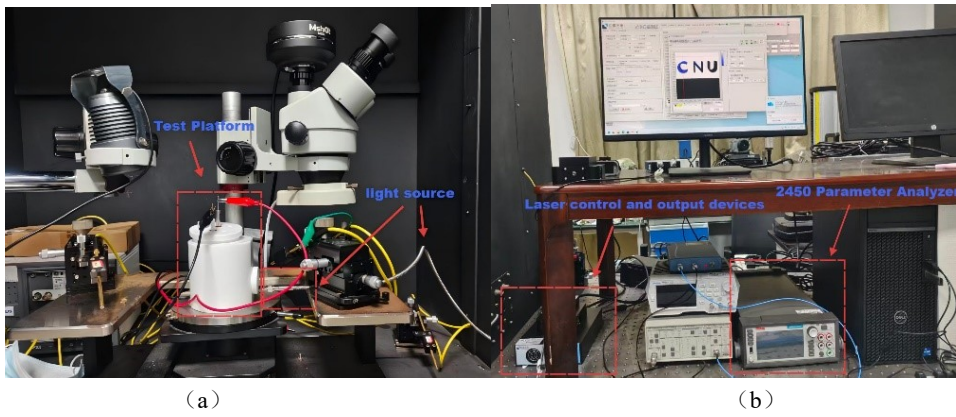


**Figure S9** (a) Schematic of the testing platform. (b) Instrumentation for laser control and data acquisition.

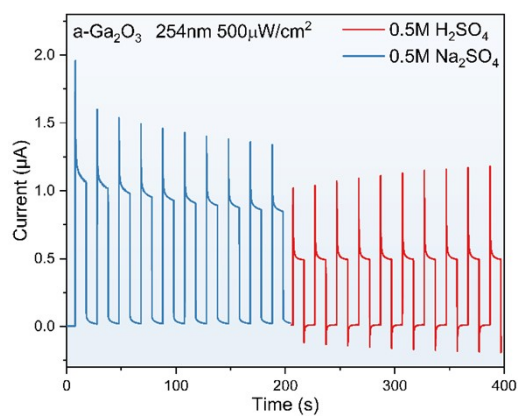


**Figure S10** I-t of the a-Ga<sub>2</sub>O<sub>3</sub> photoelectrode in neutral and acidic electrolytes.

**Table S1** Performance benchmarking of Ga<sub>2</sub>O<sub>3</sub>-based materials for ultraviolet photodetection in recent literature.

<b>Materials</b>	<b>R</b>	<b>D*</b>	<b>T<sub>r</sub>/T<sub>d</sub></b>	<b>reference</b>
<b>β-Ga<sub>2</sub>O<sub>3</sub>@α-Ga<sub>2</sub>O<sub>3</sub></b>	48.4 mA/W	8.0 × 10 <sup>11</sup>	125 ms/160 ms	[1]
<b>γ-Ga<sub>2</sub>O<sub>3</sub></b>	5.22 mA/W	3.12 × 10 <sup>11</sup>	0.35 s/0.32 s	[2]
<b>α-Ga<sub>2</sub>O<sub>3</sub>/Cu<sub>2</sub>O</b>	4.57 mA/W	2.107 × 10 <sup>9</sup>	0.815 s/0.978 s	[3]
<b>Sn doped β-Ga<sub>2</sub>O<sub>3</sub></b>	63.79 mA/W	9.58 × 10 <sup>11</sup>	1.01 s/0.19 s	[4]
<b>α-Ga<sub>2</sub>O<sub>3</sub>/Nb<sub>2</sub>CT<sub>x</sub></b>	35.4 mA/W	2.6 × 10 <sup>11</sup>	0.2 s/0.1 s	[5]
<b>β-Ga<sub>2</sub>O<sub>3</sub></b>	1.7 A/W	\	2.2 s/2.2 s	[6]
<b>Mg-doped α-Ga<sub>2</sub>O<sub>3</sub></b>	34.54 mA/W	6.36 × 10 <sup>11</sup>	0.29 s/0.14 s	[7]
<b>α-Ga<sub>2</sub>O<sub>3</sub>/MoS<sub>2</sub></b>	33.03 mA/W	2.46 × 10 <sup>11</sup>	24 ms/51 ms	This work

## REFERENCES

- [1] Y. Feng, L. Lv, H. Zhang, L. Ye, Y. Xiong, L. Fang, C. Kong, H. Li and W. Li, Catalyst-Free  $\beta$ -Ga<sub>2</sub>O<sub>3</sub>@ $\alpha$ -Ga<sub>2</sub>O<sub>3</sub> Core–Shell nanorod arrays grown on Si substrate for High-performance self-powered solar-blind photoelectrochemical photodetection, *Applied Surface Science*, 624 (2023) 157149.
- [2] Y. Sun, Y. Wei, M. Li, Y. Zhang, X. Li, L. Fan and Y. Li, Wet Chemical Synthesis of Ultrathin  $\gamma$ -Ga<sub>2</sub>O<sub>3</sub> Quantum Wires Enabling Far-UVC Photodetection with Ultrahigh Selectivity and Sensitivity, *The Journal of Physical Chemistry Letters*, 15 (2024) 4301-4310.
- [3] P. Han, T. Kang, W. Chen, M. Gao, F. Teng, P. Hu and H. Fan, Cu<sub>2</sub>O quantum dots modified  $\alpha$ -Ga<sub>2</sub>O<sub>3</sub> nanorod arrays as a heterojunction for improved sensitivity of self-powered photoelectrochemical detectors, *Journal of Alloys and Compounds*, 952 (2023) 170063.
- [4] J. Tang, Z. Yang, X. Song, X. Sha, Z. Shi, X. Zhang, A. Xiong and C. Jiang, Highly responsive and stable self-powered solar-blind photodetectors based on Sn doped  $\beta$ -Ga<sub>2</sub>O<sub>3</sub> nanorod arrays, *Journal of Materials Chemistry C*, 13 (2025) 18338-18349.
- [5] Y. Liu, Q. Gao and X. Wang, Construction of  $\alpha$ -Ga<sub>2</sub>O<sub>3</sub>/Nb<sub>2</sub>CT<sub>x</sub> heterojunction for self-powered photoelectrochemical solar-blind ultraviolet photodetectors, *Materials Science in Semiconductor Processing*, 202 (2026) 110201.
- [6] H. Zhou, H. Wang, J. Ma, B. Li, H. Xu and Y. Liu, High-performance solar-blind imaging photodetectors based on micrometer-thick  $\beta$ -Ga<sub>2</sub>O<sub>3</sub> films grown by thermal oxidation of gallium, *Journal of Materials Chemistry C*, 13 (2025) 793-801.
- [7] X. Zhou, L. Ye, L. Yuan, D. Zhang, H. Zhang, D. Pang, Y. Tang, H. Li, W. Li and H. Zeng, Mg-doped  $\alpha$ -Ga<sub>2</sub>O<sub>3</sub> Nanorods for the Construction of Photoelectrochemical-Type Self-Powered Solar Blind UV Photodetectors and Underwater Imaging Application, *Advanced Science*, 12 (2025) 2413074.